Int. J. Pharm. Investigation, 2026; 16(1):232-240.
https://www.jpionline.org

Original Article

A Correlation of Molecular Docking and ADME Studies on 5,5-diphenylimidazolidine-2,4-dione: Inhibitors of Human Voltage-Gated Sodium Channel (Nav1.2)-2KAV

Pooja Anil Nikam[1], Shabnam Babu Shaikh[2], Girish Ravindra Kokate[1], Vanita Baban Katore[3], Saiprasad Vasant Wani[1], Sabafarin Hasin Shaikh[4], Rohit Jaysing Bhor[1,*]

[1]Department of Pharmaceutical Chemistry, Pravara Rural College of Pharmacy Pravaranagar, Tal-Rahata, Ahmednagar, Maharashtra, INDIA.
[2]Department of Pharmaceutical Chemistry, Dr. Kolpe Institute of Pharmacy, A/P: Kolpewadi, Tal-Kopargaon, Ahilyanagar, Maharashtra, INDIA.
[3]Department of Pharmaceutical Chemistry, Vidya Niketan Institute of Pharmacy and Research Centre, Bota, Sangamner, Ahilayanagar, Maharashtra, INDIA.
[4]Department of Pharmaceutical Chemistry, Valmik Naik College of Pharmacy, Telwadi, Maharashtra, INDIA.

ABSTRACT

Background: The purpose of this work is to use Lipinski's rule to perform molecular docking and drug-likeness analysis of the proposed 5,5-diphenylimidazolidine-2,4-dione. One description claims that the most common chronic brain disorder is epilepsy. One typical indication of epilepsy is uncontrollable convulsions caused by temporary neuronal discharges. Many new anticonvulsants have been introduced to the Indian market, however despite the use of both new and old medications, many types of seizures have not yet been well managed with fewer adverse effects. **Materials and Methods:** Molecular Design Suite was used to conduct Combi Lab investigations and 3D-QSAR. Schrodinger Maestro was used for the molecular docking investigation. **Results:** In a combinatorial approach, three compounds (CA1-CA10) out of ten compounds showed better predicted biological activity than the most active molecule in the dataset. The amino acid residues on the human voltage-gated sodium channel (Nav1.2)-2KAV showed proximal interaction with these substances. **Conclusion:** The drug-like properties of the suggested compounds were expected. All of the suggested compounds had good molecular docking and *in silico* ADME properties, and tests were conducted to determine their capacity to inhibit the Human Voltage-gated Sodium Channel (Nav1.2)-2KAV. According to molecular docking studies, all medications seemed to bind more positively with the target protein; these pharmaceuticals could be potent sodium channel inhibitors that function via a GABAergic route. 5,5-diphenylimidazolidine-2,4-dione analogs may be equally hazardous and potent anticonvulsants. GABAergic pathway production depends on the human voltage-gated sodium channel (Nav1.2)-2KAV, one of the key enzymes.

Keywords: Convulsion, ADMET, Molecular docking, Human Voltage-Gated Sodium Channel (Nav1.2)-2KAV.

Correspondence
Dr. Rohit Jaysing Bhor
B-10, Lane 2, Musale Vasti, Hasanapur Road, Loni (B.K.), Rahata, Ahmednagar, Maharashtra, INDIA.
Email: rohit.bhor69@gmail.com
ORCID: 0000-0002-7979-3765

Received: 26-04-2025;
Revised: 18-06-2025;
Accepted: 06-08-2025.

INTRODUCTION

One of the most prevalent neurological conditions that affect people of all ages is epilepsy, sometimes known as seizures. Eighty percent of them were found to reside in low- to middle-income nations. On the other hand, epilepsy is an uncontrollable neurological seizure. It occurs when the prevalence of all chronic illnesses is seven times greaterx (Thénot *et al*., 1988; Holm and Goa, 2000). According to earlier studies, the United States spends around $15.5 billion annually on medical treatment, including epilepsy. Because epilepsy affects so many people in the US and India, it is critical to develop safer and more effective anticonvulsant medications to lower the expense of treating epilepsy. Many nations have undertaken a great deal of work to find innovative, safe, and efficient medications to treat epilepsy (Hoehns and Perry, 1993; Quera-Salva *et al*., 1994). Epilepsy comes in a variety of forms, including clonic seizures, absence seizures, and focal or generalized seizures. These days, focal seizures are treated with newly developed anticonvulsants. People of all ages are susceptible to epilepsy, sometimes referred to as seizures, which is a common neurological disorder. Eighty percent of them live in low- to middle-income nations, it was found. Conversely, epilepsy is a neurological disorder marked by uncontrolled seizures (Salvà and Costa, 1995). It happens seven times as often as the average for all chronic conditions. Prior

DOI: 10.5530/ijpi.20260371

research indicates that the cost of healthcare in 2023-24 in the United States, including epilepsy, is around $15.5 billion. Because treating epilepsy is so expensive in the US and India, there is a pressing need for safer and more potent anticonvulsant drugs. Numerous nations have worked tirelessly to find novel, secure, and efficient drugs to treat epilepsy. There are many different types of epilepsy, such as clonic seizures, absence seizures, and focal or generalized seizures (Pons *et al*., 1989). Uncontrollable convulsions brought on by excessive transient neuronal discharges were used to diagnose epilepsy (Bortoli *et al*., 2019; Yousefsani *et al*., 2020; Pick *et al*., 2005). In the wide etiology of epilepsy or seizures syndrome, a large body of research seems to suggest that several mechanisms are responsible for the many seizures. The action potential depolarization phase in excitable cells served as evidence for it. During the action potential's depolarization phase, the first inward current in cells is caused by the HVSC (Nav1.2)-2KAV (García-Santos *et al*., 2004). Additionally, a decrease in GABAergic transmission and an increase in glutamatergic neurotransmission are associated with the HVSC (Nav1.2)-2KAV, both of which are implicated in physiological issues. People suffer from epileptic seizures as a result. Our group has been synthesizing and analyzing a wide range of structurally varied anticonvulsant active stereoisomer derivatives for more than 20 years (Garcia loía-lópez *et al*., 2021). The design of new medicinal molecules depends heavily on computational biology and bioinformatics, which can also speed up the drug development process. In this work, we examine how important details about drug-receptor interactions may be uncovered by molecular docking of a drug molecule with a receptor (Mizushima and Kobayashi, 1968). Approximately 160 naturally occurring alkaloids, including 5,5-diphenylimidazolidine-2,4-dione and its derivatives, are the building blocks of heterocyclic compounds. These alkaloids are extracted from microorganisms, plants, and animals. 5,5-diphenylimidazolidine-2,4-dione has antibacterial, anti-inflammatory, antimalarial, anticonvulsant, antihypertensive, anti-diabetic, PARP inhibitory, and anticancer properties under its pharmacological action. In this study, we compute log P, solubility, drug similarity, volume, drug score, and number of Lipinski's rule violations (Garcia loía-lópez *et al*., 2021). CAiss ADME, a theoretical *in silico* ADME prediction study, was applied to all derivatives of 5,5-diphenylimidazolidine-2,4-dione. The physicochemical, pharmacokinetic, lipophilic, and drug-likeness characteristics of each derivative were assessed using a variety of descriptors (Sakat *et al*., 2010). The Chemsketch program is used to draw the molecules' 2D and 3D structures for analysis. The CAiss ADME program was utilized to calculate the ADME characteristics after converting the 2D and 3D structures of the created derivatives. The following is a list of the derivatives that were given in Figure 1 and Table 1.

MATERIALS AND METHODS

Data set

It was found using the Site Finder module that included with MOE. An alpha sphere, also known as an alpha center, is a collection of imaginary atoms. Both "hydrophilic" and "hydrophobic" were used to describe it. While the hydrophobic alpha sphere represents an area active in hydrophobic interactions, the hydrophilic alpha sphere represents a region best suited for hydrogen bond formation (Yousefsani *et al*., 2020). The protein being studied is HVSC (Nav1.2)-2KAV. We use the Autodock Vina program to study molecular docking. The positions' that the ligand docked in the pockets is most likely to favor are those that yield the greatest binding scores. The complex's with the highest score for the ligand at a certain site was selected for further analysis out of ten top-score's docking postures that were produced. The Protein Data Bank supplied the Ribbon Structure structures for HVSC (Nav1.2)-2KAV (Nav1.2)-2KAV. Auto dock version was 1.5.6. Chain A was chosen. Polar hydrogens and Gasteiger charges were then introduced after the water was removed (Hasanvand *et al*., 2018). They decided on a grid map. The compounds' 2D formula was drawn using ChemDraw Ultra 12.0. Avogadro software was used to minimize energy use. Autodock Vina was used to realize the docking process, while Discovery Studio 3.5 was used to visualize the interactions. CeleHVSC (Nav1.2)-2KAV ib (CEL) crystal structures were compared to the anticipated conformations of docking data in order to optimize the docking method.

Calculation of the molecular descriptors

Each molecule's 2D molecular arrangement was created using sketch and view tools, and it was subsequently transformed into the 3D biochemical structure of several derivatives. In order to get accurate and reliable data on the electrical properties of the molecules, calculations were made for BBB perm. (log BBB), GI absorption, PPB (%), and Caco2 permeability (log Papp in10-6 cm/s). infringement of the Lipinski, who rule, the coefficient of mass conservation rule, Mol Log P, and the donor and acceptor values for the H bond(Das & Chatterjee, 1995). The 10 molecular descriptors that were calculated for the data set are listed in Table 1. The active amino residues, bond length, bond category, bond type, ligand energies, and docking scores properties of 5,5-diphenylimidazolidine -2,4-dione were given in Table 4.

In silico ADME

ADME, is the study of the pharmacokinetics of materials inside living things. ADME assesses the risk of administering a medicine to humans or other animals(Yesmin *et al*., 2020). The pharmacokinetic properties of new 5,5-diphenylimidazolidine-2,4-dione derivatives are determined *in silico* using an online tool such as CAiss ADME (http://www.CAissadme.ch/). Lipinski's rule is currently being studied. Along with hydrophobicity,

hydrogen bonding buildings, electronic variation, versatility, and molecule size, this encompasses a wide range of pharmocophore attributes, such as transport properties, bioavailability, reactivity, affinity to proteins, toxicity, stability of metabolism, and many more(Jia *et al*., 2022). Druglikeness analysis of designed 5,5-diphenylimidazolidine -2,4-dione with Lipinski's rule and *In silico* ADMET (Absorption, Distribution, Metabolism, Excretion, and Toxicity) properties of 5,5-diphenylimidazolidine -2,4-dione were given in Tables 2 and 3.

RESULTS

HVSC (Nav1.2)-2KAV enzymes were docked with the drugs, and the molecular interactions between them were examined. Table 4 summarize interactions between chemicals with residues of dynamic amino acids, whereas Figures 2-4 display the 2D-3D conformations for molecular bindings. Computer-Aided Molecular Design (CAMD) has traditionally concentrated on lead optimization and identification, and several creative techniques have been created to help increase the binding affinities of drug candidates to certain receptors. QSAR is one such technique that was covered in the previous chapter. This chapter will cover the newly developed idea of "drug-likeness" as well as the computer modelling of a number of biological and physicochemical characteristics that are crucial in turning a clinical lead into a commercially available medication. Pharmacologists and medicinal chemists have looked for beneficial drug-like chemical characteristics that produce agents with predictable oral therapeutic effectiveness. Drug development process follows Lipinski's "rule of five" which is computational and experimental method for estimating solubility, permeability. Those are general guideline which assesses drug-likeness and establishes whether molecule has pharmacological activity. The rule was founded on the finding that the majority of medications that work well when taken orally are tiny, somewhat lipophilic molecules. The toxicity of a ligand is thought to be required to ligand as function to effective discovery tool, and Qik-Prop produces physically relevant descriptions. The Ligprep module used for ligand preparation utilized in investigation. The protein preparation wizard utilized for protein preparation. The PDB data bank provided the X-ray crystal structures of HVSC (Nav1.2)-2KAV. The grid generated using Receptor Grid Generation Wizard. Receptor Grid Generation Wizard were given in Figure 4 Glide XP coupled the ligand with the protein, and the interactions were seen. Based on the optimal ligand-protein interaction, the scoring function assigns points. The extra-precision mode was used to assess the docking positions. The program detects steric conflicts, metal-ligation interactions, hydrophobic interactions, and hydrogen bonding. Every substance has a molecular weight between 400 and 500, which is less than 500. The compounds' computed log P values fall between 3.56-5.35. The substances being studied have donors of hydrogen bonds.

In silico ADMET

Good ADMET property prediction techniques are becoming more and more necessary to achieve two main goals. In order to lower the risk, novel compounds libraries should be designed first. Secondly, screening and testing should be optimized by focusing on the most promising compounds. Predicting characteristics like oral absorption, bioavailability, BBB penetration, clearance, and Vd (for frequency) which give information about dosage quantity and frequency is our goal. Molecular modelling and data modelling are the two categories of computational techniques that are employed. Molecular modelling utilizes quantum techniques to evaluate possibility of interaction, including cytochrome P450s, which has role in ADME processes. QSAR techniques is commonly used for data modelling. These look for relationships between a collection of chemical and structural molecules likes GI absorption; BBB permeant; Pgp substrate; CYP1A2 inhibitor; CYP2C19 inhibitor; CYP2C9 inhibitor; CYP2D6 inhibitor; and CYP3A4 inhibitor in question and certain property using statistical methods. Choosing appropriate mathematical method, appropriate chemical descriptors for ADMET endpoint, sizable

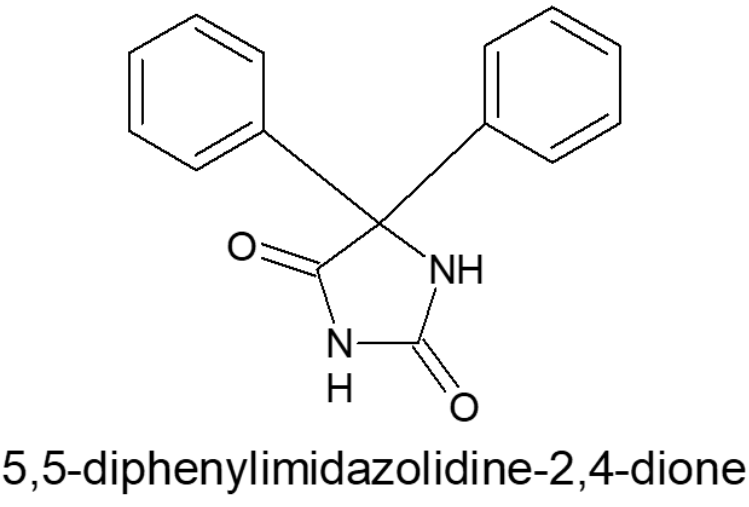

Figure 1: Designed 5,5-diphenylimidazolidine -2,4-dione.

Table 1: Derivatives of designed compound of 5,5-diphenylimidazolidine -2,4-dione.

Label	Structure
CA1	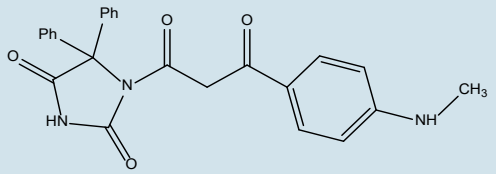
CA2	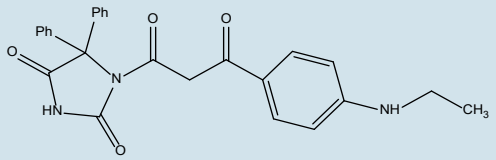
CA3	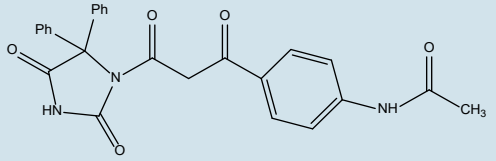
CA4	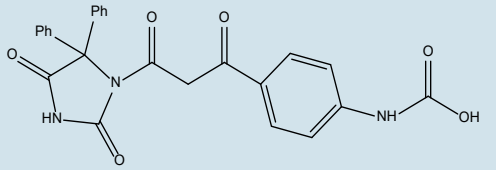
CA5	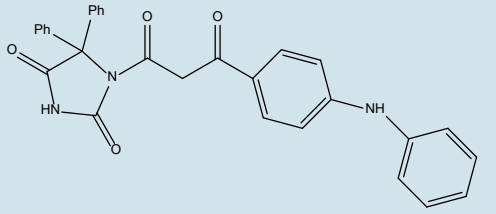
CA6	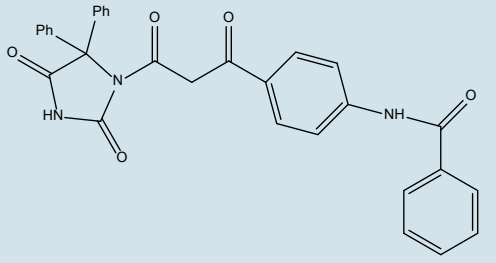
CA7	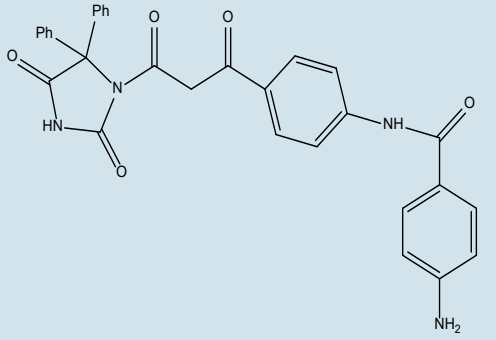
CA8	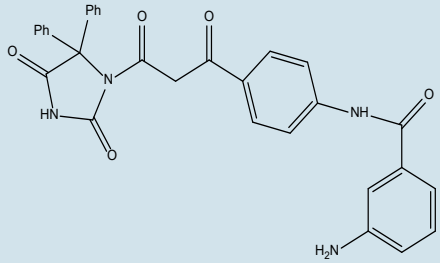
CA9	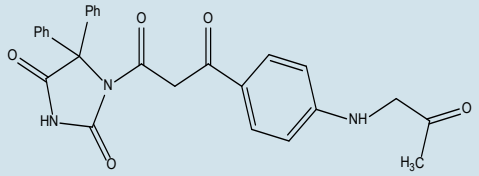
CA10	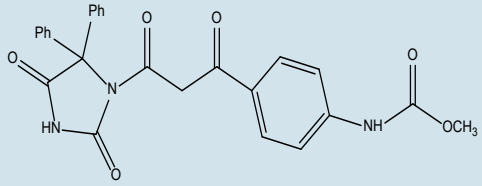

enough collection of data pertaining with same endpoint for model validation are all essential components of effective prediction models for ADMET parameters. Recent developments in the prediction of ADME-related physicochemical qualities (like lipophilicity), ADME properties (like absorption), and toxicity problems (like drug-drug interactions) are discussed in this article see Table 3. During the next ten years or so, automated medium and HTS *in vitro* tests will be employed. The derivatives of 5,5-diphenylimidazolidine-2,4-dione are effectively docked into the active site of the target protein, namely the human voltage-gated sodium channel (Nav1.2)-2KAV, using autodock software. All of the compounds in this study are active, however CA9 and CA7 are the most active with the lowest binding affinity, making them efficient inhibitors. This is in contrast to CA1, CA2, CA3, CA5, CA7, CA9, and CA10, which show hydrophobic bonding. CA9 and CA7 have distinct hydrophobic interactions with MET110, VAL132, PHE109, ALA293, ILE431, and TYR107. Furthermore, as Tables 2 and 3 demonstrate, the formation of hydrogen bonds between the molecules TYR and VAL is generally accepted. Docking experiments shown how the most potent compounds bind to both the target protein and the designer molecule. The 2D and 3D structures of the suggested 5,5-diphenylimidazolidine-2,4-dione derivatives of CA7 and CA9 are displayed below (Table 4).

Table 2: Druglikeness analysis of designed 5,5-diphenylimidazolidine -2,4-dione with Lipinski's rule.

Comp.	Molecular weight (g/mol)	CMC rule violation	Lipinski's rule violation	Mol Log P	H bond donor	H bond acceptor	No. of rotatable bonds	TPSA (Å2)
CA1	422.86 g/mol	0	Yes	2.95	1	4	6	83.55 Å²
CA2	432.44 g/mol	0	Yes	2.68	1	4	6	83.55 Å²
CA3	447.51g/mol	0	Yes	2.40	1	6	7	129.37 Å²
CA4	436.46 g/mol	0	Yes	2.88	1	4	7	83.55 Å²
CA5	487.31 g/mol	0	Yes	3.05	1	4	6	83.55 Å²
CA6	439.48 g/mol	0	Yes	3.15	1	4	6	83.55 Å²
CA7	438.44g/mol	0	Yes	2.15	1	5	7	92.78 Å²
CA8	378.41g/mol	0	Yes	2.47	1	4	6	83.55 Å²
CA9	426.40g/mol	0	Yes	2.84	1	5	6	83.55 Å²
CA10	433.42 g/mol	0	Yes	1.81	1	5	6	107.34 Å²

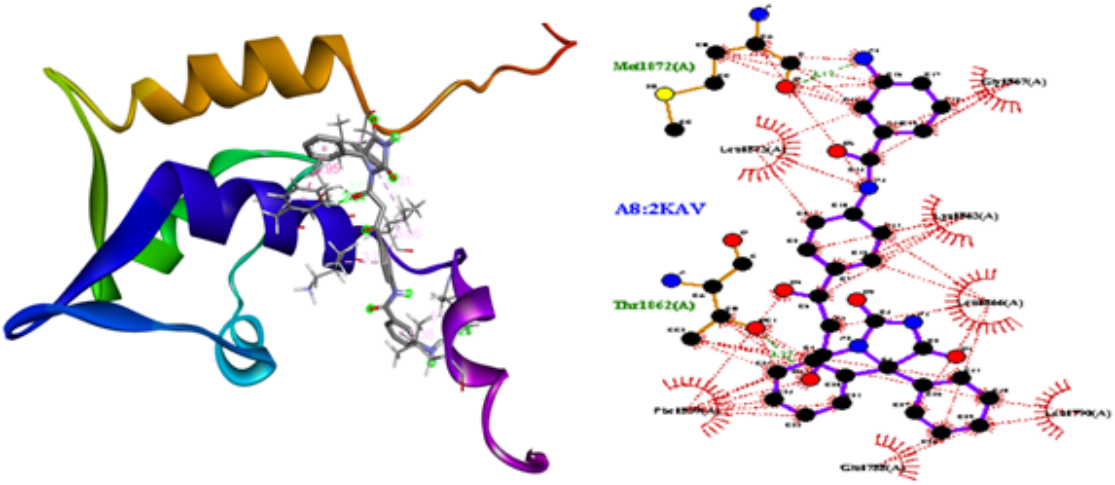

Figure 2: 2 D and 3 D Structure of designed 5,5-diphenylimidazolidine -2,4-dione derivatives of CA7 are given above.

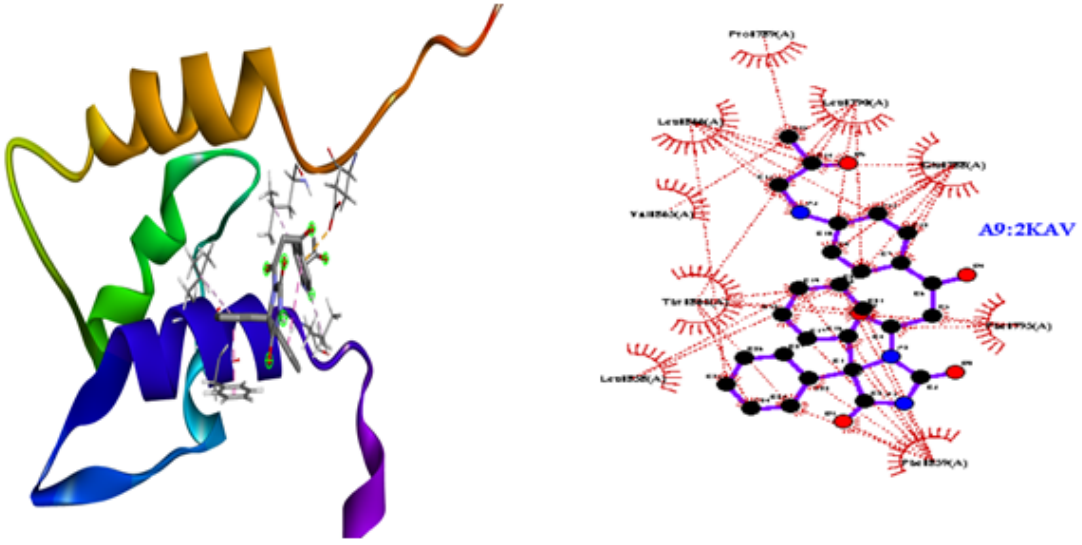

Figure 3: 2 D and 3 D Structure of designed 5,5-diphenylimidazolidine -2,4-dione derivatives of CA 8 are given above.

Table 3: *In silico* ADMET (Absorption, Distribution, Metabolism, Excretion, and Toxicity) properties of 5,5-diphenylimidazolidine -2,4-dione.

Comp.	Absorption		Distribution			Metabolism				
	Caco2 permeability (log Papp in10-6 cm/s)	GI absorption	BBB perm. (log BBB)	BBB	PPB (%)	(Nav1.2)-2KAV A4 substrate	(Nav 1.2)-2KAV inhibitor	(Nav 1.3)-2KAV inhibitor,	(Nav 1.4)-2KAV inhibitor	(Nav 1.5)-2KAV inhibitor
CA1	22.076	High	0.486381	No	93.768450	Weakly	No	Yes	No	Yes
CA2	21.0161	High	0.844468	No	100	Weakly	No	Yes	No	Yes
CA3	20.1602	High	0.0168724	No	96.853275	Weakly	No	Yes	No	Yes
CA4	21.1528	High	0.392584	No	99.451925	Weakly	No	Yes	Yes	Yes
CA5	22.0535	High	98.262119	No	0.496217	Weakly	No	Yes	No	Yes
CA6	21.3996	High	0.126686	No	95.363582	Weakly	No	Yes	No	No
CA7	21.5709	High	0.653444	No	100	Non	No	Yes	Yes	Yes
CA8	21.0078	High	1.78546	No	100	Weakly	No	Yes	No	Yes
CA9	21.6812	High	0.420994	No	96.096212	Weakly	No	Yes	No	Yes
CA10	20.6545	High	0.0819447	No	100	Weakly	No	Yes	No	Yes

DISCUSSION

All of the "compounds had molecular weights less than 500," according to data warrior results, suggesting that they will bind action site. All drugs had LogP below 5, which indicates excellent penetration and absorption across cell membranes. Table 1 provides various derivatives of imidazolidine-2,4-dione which specifics on the "binding energies and hydrogen bonds" of CA1-CA10. Furthermore, the dock score values of all the produced compounds ranged from 7.5 and 8.8 kcal/mol, suggesting their binding energies lower to imidazolidine-2,4-dione, which has "binding energy" of 8.0 kcal/mol. Analogues with best interactions and far from zero auto dock score determined as best conformation. Both complexes' RMSD plot analysis revealed that the CA9-protein complex had a stable trajectory for more research after achieving excellent stability at 100 ns. Analysis of the synthetic imidazolidine-2,4-dione derivatives. Interactions towards HVSC (Nav1.2)-2KAV i.e. Human Voltage-gated Sodium Channel (Nav1.2)-2KAV that they have anti-inflammatory properties. Phe381, Leu-384, Tyr-385, Trp-387, Phe-518, Gly-526, Met-522, Tyr348, Val-349, Leu-352 were active amino acids in HVSC (NAV1.2)-2KAV. CA5 and CA6 demonstrated Pi-Pi stacking to TYR355: HH; SER530:HG; SER530:HB1; TYR355; PHE381; TYR385; TRP387; TRP387; TRP387; ALA527:N; LEU384; MET522; VAL349; ALA527; and LEU531 via the imidazolidine-2,4-dione and H-bond with Ser-530 via nitrogen of the imidazolidine-2,4-dione ring. CA15 demonstrated Pi-Pi stacking with Tyr385 via the imidazolidine-2,4-dione ring and hydrogen bonding with Ser530. CA11 demonstrated Pi-Pi stacking with ARG120:HH11; ARG120:HH12; TYR355:HH; ARG120:NH1; ARG120:NH2; VAL89; VAL116; VAL349; ALA527; VAL349 and LEU352; ALA527 via benzene ring and H-bond with Met-522 via nitrogen. Comparing the 10 imidazolidine-2,4-dione derivatives to the standard drug(-10.705 kcal/mol), CA1 and CA2 had a satisfactory docking score of -8.572 kcal/mol. ARG120:HH11; ARG120:HH12; TYR355: HH; ARG120:NH1; ARG120:NH2; VAL89; VAL116; VAL349; ALA527;VAL349 and LEU352; ALA527, were active amino acids in the enzyme HVSC (NAV1.2)-2KAV enzymes. CA5 demonstrated H-Bond with TYR355: HH; SER530:HG; SER530:HB1; TYR355; PHE381; TYR385; TRP387; TRP387; TRP387; ALA527:N; LEU384; MET522; VAL349; ALA527; and LEU531 nitrogen of imidazolidine-2,4-dione and Pi-Pi stacking with Tyr-385 via benzene. CA demonstrated Pi-cation interaction to TYR355:HH; SER530: HG; SER530:HB1; PHE381; TYR385; TRP387; TRP387; TRP387; VAL116; LEU359; LEU531; LEU384; MET522; VAL349; ALA;527 and LEU531 via imidazolidine-2,4-dione and Pi-pi stacking with Tyr-385 and Trp-387 via benzene. CA9 demonstrated H-bond with ARG120:HH12; ARG120:NH1; LEU93; VAL116; VAL116; VAL349; ALA527; LEU352 and Ser-530 via imidazolidine-2,4-dione and Pi-Pi stacking with Tyr-385. Comparing 10 imidazolidine-2,4-dione derivatives to the standard drug(-10.099 kcal/mol), (CA6), (CA7), (CA8), and (CA9) showed elevated docking scores, from -8.25 to -8.51 kcal/mol. Compound CA5's binding affinity score with HVSC (NAV1.2)-2KAV is -56.79 kcal/mol, whereas compound CA6's binding score with HVSC (NAV1.2)-2KAV is -60.27 kcal/mol. Late-stage drug attrition may now be decreased and the most promising compounds can be found using *in silico* ADME screens. To have a good *in vivo* response, pharmacodynamic and pharmacokinetic characteristics must be balanced. Further details on medication dose and regimen are also provided by ADMET. According to “Lipinski's rule of five”, an oral medication is selected if its molecular weight is < 500, hydrogen bond donors is less than five, hydrogen bond acceptors is less than ten, and log P value less than five. Oral bioavailability depends on molecular flexibility, which is

Table 4: The active amino residues, bond length, bond category, bond type, ligand energies, and docking scores properties of 5,5-diphenylimidazolidine -2,4-dione.

Active Amino acid	Bond length	Bond Type	Bond Category	Ligand Energy	Docking score
			CA7		
THR1862	2.98962	Hydrogen Bond	Conventional Hydrogen Bond	23.9714 kcal/mol	-8.6
GLU1788	3.96814	Electrostatic	Pi-Anion		
PHE1859	4.27965	Hydrophobic	Pi-Pi Stacked		
LYS1863	3.81151	Hydrophobic	Pi-Alkyl		
LEU1866	5.09554	Hydrophobic	Pi-Alkyl		
MET1872	5.19609	Hydrophobic	Pi-Alkyl		
LEU1875	5.16303	Hydrophobic	Pi-Alkyl		
LEU1790	4.68783	Hydrophobic	Pi-Alkyl		
LEU1866	4.92985	Hydrophobic	Pi-Alkyl		
CA8					
THR1862	2.53729	Hydrogen Bond	Conventional Hydrogen Bond	24.0817 kcal/mol	-9.1
MET1872	2.25325	Hydrogen Bond	Conventional Hydrogen Bond		
THR1862	3.02017	Hydrogen Bond	Carbon Hydrogen Bond		
PHE1859	3.95053	Hydrophobic	Pi-Pi Stacked		
LYS1863	3.72923	Hydrophobic	Pi-Alkyl		
LEU1866	5.05964	Hydrophobic	Pi-Alkyl		
MET1872	5.0483	Hydrophobic	Pi-Alkyl		
LEU1875	5.37837	Hydrophobic	Pi-Alkyl		
LEU1790	4.96091	Hydrophobic	Pi-Alkyl		
LEU1866	5.30535	Hydrophobic	Pi-Alkyl		
			CA9		
GLU178	3.24832	Electrostatic	Pi-Anion	17.0305 kcal/mol	-7.4
PHE1859	3.72378	Hydrophobic	Pi-Pi Stacked		
UNL1	4.66336	Hydrophobic	Pi-Pi Stacked		
LEU1858	5.05451	Hydrophobic	Pi-Alkyl		
LEU1790	4.68346	Hydrophobic	Pi-Alkyl		
LEU1866	5.24226	Hydrophobic	Pi-Alkyl		
			CA10		
GLU18; MET1872	4.87786	Hydrophobic	Amide-Pi Stacked	14.7254 kcal/mol	-7.4
LYS1863	4.35358	Hydrophobic	Alkyl		
LEU1866	4.66732	Hydrophobic	Alkyl		
PHE185	5.38689	Hydrophobic	Pi-Alkyl		
ARG1864	4.08295	Hydrophobic	Pi-Alkyl		
MET1842	4.87229	Hydrophobic	Pi-Alkyl		
ALA1860	5.09937	Hydrophobic	Pi-Alkyl		
ARG1864	4.92534	Hydrophobic	Pi-Alkyl		
LYS1863	3.66599	Hydrophobic	Pi-Alkyl		
LEU1866	5.37564	Hydrophobic	Pi-Alkyl		

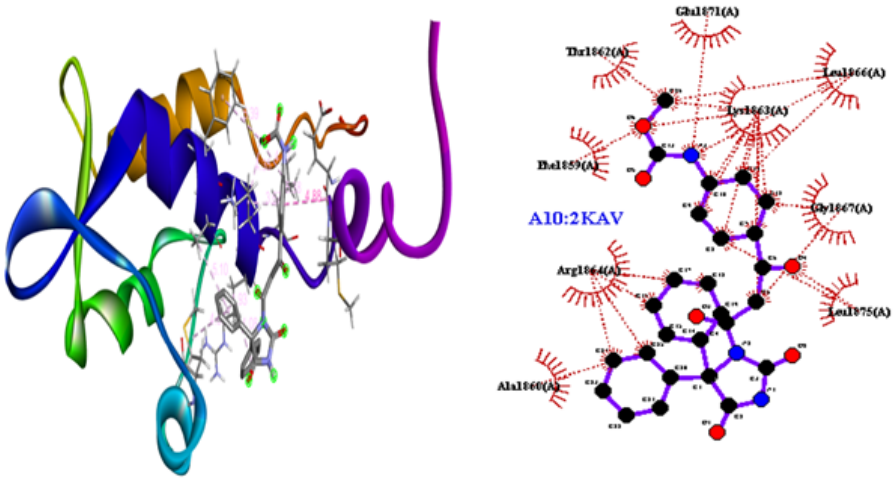

Figure 4: 2 D and 3 D Structure of designed 5,5-diphenylimidazolidine -2,4-dione derivatives of CA10 are given above.

shown by the number of rotatable bonds. Additionally, as TPSA is indirectly related to percentage absorption, it suggested that used as 3D descriptor in number of hydrogen bonding groups. They should thus have high oral absorption; nevertheless, this quality cannot be used to explain variances in bioactivity. Additionally, the compounds' oral absorption percentage ranged from 70.69 to 73.87%, indicating high ADME. Their TPSA values were 101.3 and 104.80 A2 (140 A2), respectively, and rotatable bonds ranged in 7 to 8 (<10). It is generally accepted that a molecule that is soluble in water and satisfies Lipinski's and Veber's criteria is said to possess both lipophilicity and hydrophilicity. Interactions towards HVSC (NAV1.2)-2KAV enzymes revealed that they have anti-inflammatory properties. TYR355: HH; SER530:HG; SER530:HB1; TYR355; PHE381; TYR385; TRP387; TRP387; TRP387; ALA527:N; LEU384; MET522; VAL349; ALA527; and LEU531 were active amino acids in HVSC (NAV1.2)-2KAV enzymes. CA13 and CA15 demonstrated Pi-Pi stacking to Tyr385 and Trp387 via the imidazolidine-2,4-dione and H-bond with Ser-530 via nitrogen of the imidazolidine-2,4-dione ring. CA3 demonstrated Pi-Pi stacking with TYR355: HH; SER530:HG; SER530:HB1; TYR355; PHE381; TYR385; TRP387; TRP387; TRP387; ALA527:N; VAL349; ALA527; and LEU531 via the imidazolidine-2,4-dione ring and hydrogen bonding with Ser530. CA14 demonstrated Pi-Pi stacking with Tyr-385 via benzene ring and H-bond with Met-522 via nitrogen. Comparing the 10 imidazolidine-2,4-dione derivatives to the standard drug (-10.705 kcal/mol), CA8 and CA9 had a satisfactory docking score of -8.572 kcal/mol. Phe381, Leu384, Tyr385, Trp387, were active amino acids in the enzyme HVSC (NAV1.2) enzymes. BI5 demonstrated H-Bond with Ser-530 nitrogen of imidazolidine-2,4-dione and Pi-Pi stacking with Tyr-385 via benzene. CA10 demonstrated Pi-cation interaction to TYR355: HH; SER530:HG; SER530:HB1; TYR355; PHE381; TYR385; TRP387; TRP387; TRP387; ALA527:N; LEU384; MET522; VAL349; ALA527; and LEU531 via imidazolidine-2,4-dione and Pi-pi stacking with Tyr-385 and Trp-387 via benzene. CA1 demonstrated H-bond with TYR355: HH; SER530:HG; SER530:HB1; TYR355; PHE381; TYR385; TRP387; TRP387; TRP387; ALA527:N; LEU384; MET522; VAL349; ALA527; and LEU531 via imidazolidine-2,4-dione and Pi-Pi stacking with Tyr-385.the docked (CA6), (CA7), (CA8), and (CA9) exhibit the strongest inhibitor. With ligand energy 23.9714 kcal/mol, CA7 forms hydrophobic contacts with THR1862, MET1872, THR1862, PHE1859, LYS1863, LEU1866, MET1872, LEU1875, LEU1790, and LEU1866, as well as hydrogen bonds with PHE and MET. With ligand energy 24.0817 kcal/mol, CA8 forms hydrophobic contacts with THR1862, GLU1788, PHE1859, LYS1863, LEU1866, MET1872, LEU1875, LEU1790, and LEU1866, as well as hydrogen bonds with PHE and MET. With a ligand energy of 17.0305 kcal/mol, CA9 forms hydrophobic contacts with GLU178, PHE1859, UNL1, LEU1858, LEU1790, LEU1866, and LEU1866, as well as hydrogen bonds with PHE and MET. With ligand energy 14.7254 kcal/mol, CA10 forms hydrophobic contacts with GLU18, MET1872, LYS1863, LEU1866, PHE185, ARG1864, MET1842, ALA1860, ARG1864, LYS1863, and LEU1866, as well as hydrogen bonds with PHE and MET.

CONCLUSION

By creating a set of ten derivatives, the *in silico* parameter of 5,5-diphenylimidazolidine-2,4-dione was examined. According to ADME studies, all produced compounds can be considered lead molecules. Every suggested molecule had a good oral bioavailability and complied with Lipinski's rule of five. The ADME investigation has demonstrated that these compounds qualify for drug-likeness. These substances have advantageous intestinal and PPB absorption properties. All of the tests point to the significant inhibitory effects of CA8 compounds on the target protein, Human Voltage-gated Sodium Channel (Nav1.2)-2KAV.

Overall, the results indicate that the antimicrobial compounds CA7, CA9, and CA8 exhibit strong inhibitory activity against Human Voltage-gated Sodium Channel (Nav1.2)-2KAV. However, a promising ADME medication-like profile for the current compounds offers the possibility of quickly adding electron withdrawing and electron donating groups with specific modifications to lead structures that enhance inhibitory activity towards the drug receptor target.

ACKNOWLEDGEMENT

The authors are thankful to Dr. S.B. Bhawar, Pravara Rural College of Pharmacy, Pravaranagar.

CONFLICT OF INTEREST

The authors declare that there is no conflict of interest.

ETHICAL APPROVAL

Animal ethical approval number was 1942/PO/Re/ S/17/CPCSE A/2022/01/09.

ABBREVIATIONS

mg/kg: Milligram/kilograms; **sec:** seconds; **kcal:** kilocalorie; **Mol. Wt:** Molecular Weight; **g:** Gram; **LEU:** Leucine; **THR:** Threonine; **ALA:** Alanine; MET: Methionine; **PHE:** Phenylalanine; **WHO:** World health Association; **Log P:** Partition Coefficient.

REFERENCES

Ayeni, E. A., Aldossary, A. M., Ayejoto, D. A., Gbadegesin, L. A., Alshehri, A. A., Alfassam, H. A., Afewerky, H. K., Almughem, F. A., Bello, S. M., & Tawfik, E. A. (2022). Neurodegenerative diseases: Implications of environmental and climatic influences on neurotransmitters and neuronal hormones activities. International Journal of Environmental Research and Public Health, 19(19), Article 12495. https://doi.org/10.3390/ijerph191912495

Bomalaski, M. N., Claflin, E. S., Townsend, W., & Peterson, M. D. (2017, September 1). Zolpidem for the treatment of neurologic disorders: A systematic review. JAMA Neurology, 74(9), 1130–1139. https://doi.org/10.1001/jamaneurol.2017.1133

Bortoli, M., Dalla Tiezza, M., Muraro, C., Pavan, C., Ribaudo, G., Rodighiero, A., Tubaro, C., Zagotto, G., & Orian, L. (2019, February 7). Psychiatric disorders and oxidative injury: Antioxidant effects of zolpidem therapy *disclosed in silico*. Computational and Structural Biotechnology Journal. PubMed: 30867894, 17, 311–318. https://doi.org/10.1016/j.csbj.2, https://www.ncbi.nlm.nih.gov/pmc/articles/PMC6396081

Chen, L., Deng, H., Cui, H., Fang, J., Zuo, Z., Deng, J., Li, Y., Wang, X., & Zhao, L. (2018). Inflammatory responses and inflammation-associated diseases in organs. Oncotarget. PubMed: 29467962, 9(6), 7204–7218. https://doi.org/10.18632/oncotarget.23208, https://www.ncbi.nlm.nih.gov/pmc/articles/PMC5805548

Das, S. N., & Chatterjee, S. (1995). Long-term toxicity study of ART-400. Indian Indg Med, 16(2), 117–123.

Durand, A., Thénot, J. P., Bianchetti, G., & Morselli, P. L. (1992). Comparative pharmacokinetic profile of two imidazopyridine drugs: Zolpidem and alpidem. Drug Metabolism Reviews, 24(2), 239–266. https://doi.org/10.3109/03602539208996294, https://pubmed.ncbi.nlm.nih.gov/1576937

Erratu, m. (2017, September 1). In JAMA Neurology, 74(9), 1144. https://doi.org/10.1001/jam aneurol.2017.2049. https://pubmed.ncbi.nlm.nih.gov/28655027

García-López, E. B., Muñoz-Ochoa, M., Hernández-Guerrero, C. J., Nieto-Camacho, A., & Band-Schmidt, C. J. (2021, August 1). Evaluation of anti-inflammatory activity of macroalgae collected from Baja California Sur, Mexico. International Journal of Pharmacy and Pharmaceutical Sciences, 13(8), 81–88. https://doi.org/10.22159/ijpps.2021v13i8.41453

García-Santos, G., Herrera, F., Martín, V., Rodriguez-Blanco, J., Antolín, I., Fernández-Marí, F., & Rodriguez, C. (2004, December). Antioxidant activity and neuroprotective effects of zolpidem and several synthesis intermediates. Free Radical Research, 38(12), 1289–1299. https://doi.org/10.1080/10715760400017343, https://pubmed.ncbi.nlm.nih.gov/15763953

Hasanvand, A., Pirzadroozbahani, N., Ahmadizar, F., Kharazmkia, A., Mir, S., Amanolahi Baharvand, P. A., Goudarzi, M., & Mohammadrezaei Khorramabadi, R. (2018). Evaluation of the antioxidant effects of zolpidem in the rat model of cisplatin-induced nephrotoxicity. Journal of Renal Injury Prevention, 7(4), 235–239. https://doi.org/10.15171/jrip.2018.54

Hoehns, J. D., & Perry, P. J. (1993, November). Zolpidem: A nonbenzodiazepine hypnotic for treatment of insomnia. Clinical Pharmacology, 12(11), 814–828. Erratum in: (1993, December). Clinical Pharmacy, 12(12), 881. https://pubmed.ncbi.nlm.nih.gov/8137604.

Holm, K. J., & Goa, K. L. (2000, April). Zolpidem: An update of its pharmacology, therapeutic efficacy and tolerability in the treatment of insomnia. Drugs, 59(4), 865–889. https://doi.org/10.2165/00003495-200059040-00014, https://pubmed.ncbi.nlm.nih.gov/10804040

Jia, Z., Wang, P., Xu, Y., Feng, G., Wang, Q., He, X., Song, Y., Liu, P., & Chen, J. (2022, September 27). Trypsin inhibitor LH011 inhibited DSS-induced mice colitis via alleviating inflammation and oxidative stress. Frontiers in Pharmacology. PubMed: 36238566, 13, Article 986510. https://doi. https://doi.org/10.3389/fphar.2022.986510, https://www.ncbi.nlm.nih.gov/pmc/articles/PMC9551103

Lamptey, R. N. L., Chaulagain, B., Trivedi, R., Gothwal, A., Layek, B., & Singh, J. (2022). A review of the common neurodegenerative disorders: Current therapeutic approaches and the potential role of nanotherapeutics. International Journal of Molecular Sciences, 23(3), 1851. https://doi.org/10.3390/ijms23031851

Langtry, H. D., & Benfield, P. (1990, August). Zolpidem. A review of its pharmacodynamic and pharmacokinetic properties and therapeutic potential. Drugs, 40(2), 291–313. https://doi.org/10.2165/00003495-199040020-00008, https://pubmed.ncbi.nlm.nih.gov/2226217

Miao, J., Ma, H., Yang, Y., Liao, Y., Lin, C., Zheng, J., Yu, M., & Lan, J. (2023, June 15). Microglia in Alzheimer's disease: Pathogenesis, mechanisms, and therapeutic potentials. Frontiers in Aging Neuroscience. PubMed: 37396657, 15, Article 1201982. https://doi.org/10.3389/fn, https://www.ncbi.nlm.nih.gov/pmc/articles/PMC10309009

Cite this article: Nikam PA, Shaikh SB, Kokate GR, Katore VB, Wani SV, Shaikh SH, *et al*. A Correlation of Molecular Docking and ADME Studies on 5,5-diphenylimidazolidine-2,4-dione: Inhibitors of Human Voltage-Gated Sodium Channel (Nav1.2)-2KAV . Int. J. Pharm. Investigation. 2026;16(1):232-40.